DEVELOPMENT OF SPECIMEN PROCESSING WORKFLOWS FOR MASS SPECTROMETRIC DETECTION AND CHARACTERIZATION OF TDP-43

by

Taylor Pobran

B.Sc., The University of Victoria, 2017

A THESIS SUBMITTED IN PARTIAL FULFILLMENT OF

THE REQUIREMENTS FOR THE DEGREE OF

MASTER OF SCIENCE

in

THE FACULTY OF GRADUATE AND POSTDOCTORAL STUDIES

(Pathology and Laboratory Medicine)

THE UNIVERSITY OF BRITISH COLUMBIA

(Vancouver)

December 2019

The following individuals certify that they have read, and recommend to the Faculty of Graduate and Postdoctoral Studies for acceptance, a thesis/dissertation entitled:

Development of specimen processing workflows for mass spectrometric detection and characterization of TDP-43

submitted by Taylor Pobran in partial fulfillment of the requirements for

the degree of Master of Science

in Pathology and Laboratory Medicine

Examining Committee:

Mari DeMarco, Pathology and Laboratory Medicine
Supervisor

Graham Sinclair, Pathology and Laboratory Medicine
Supervisory Committee Member

Joerg Gsponer, Biochemistry and Molecular Biology
Supervisory Committee Member

Bruce McManus, Pathology and Laboratory Medicine
Additional Examiner

Additional Supervisory Committee Members:

Dana Devine, Pathology and Laboratory Medicine
Supervisory Committee Member

Abstract

Transactive response DNA-binding protein 43 kDa (TDP-43) is a highly conserved protein that regulates nucleic acid processing. In humans, TDP-43 is widely expressed across different tissues in the body. In frontotemporal dementia and amyotrophic lateral sclerosis, two progressive neurodegenerative diseases, TDP-43 forms insoluble aggregates in central nervous tissues. Unfortunately, there is no cure for these diseases and a definitive diagnosis can only be made upon autopsy. As such, there is great interest in detecting, characterizing and quantifying TDP-43 and its disease-related post-translational modifications to investigate pathogenesis and as a potential biomarker.

Characteristic TDP-43 post-translational modifications of TDP-43 deposits in frontotemporal dementia and amyotrophic lateral sclerosis include ubiquitination, hyper-phosphorylation, and proteolytic fragmentation. These pathological deposits have been primarily characterized by immunometric methods, namely western blot analysis, and thus methods with greater structural resolution are needed to aid in our understanding of the pathological processes associated with TDP-43 misfolding and aggregation. Detailed analysis of TDP-43 in human tissues and biofluids is hindered by sample complexity and the relatively low abundance of TDP-43.

The aims of this thesis were thus to (1) develop a selective and multiplex method for the detection and characterization of TDP-43 using liquid chromatography-tandem mass spectrometry (LC-MS/MS), and (2) develop protocols for enrichment of TDP-43 from human fluids, tissues and cells to improve analytical sensitivity. Application of the LC-MS/MS method

enabled detection and characterization of TDP-43 in biological matrices including human cell lines and human brain tissue. In addition, aptamer enrichment of endogenous TDP-43 from these biological matrices led to improved signal-to-noise ratios and increased sequence coverage, when coupled to the LC-MS/MS method. This targeted multiplex mass spectrometric provides the opportunity for characterization of pathological forms of TDP-43 at higher resolution compared to ligand binding methods.

Lay Summary

In frontotemporal dementia (FTD) and amyotrophic lateral sclerosis (ALS), clusters of a protein named TDP-43, form inside nerve cells of the brain and/or spinal cord. While all humans have the TDP-43 protein in their cells, the clusters of TDP-43 are not found in healthy individuals. Thus, there is interest in studying TDP-43 to gain a better understanding of the cause of FTD and ALS. Studying TDP-43 can be challenging as it is found in most human tissues and biofluids. The objectives of this thesis were to develop a process that can isolate TDP-43 from these complex tissues and fluids, allowing for detailed examination of this protein. This new way to investigate the disease forms of TDP-43 found in FTD and ALS aims to improve our understanding of these diseases and develop biofluid tests to diagnose FTD and ALS.

Preface

The following work presented was conducted as part of the research group of Dr. Mari L. DeMarco in the Department of Pathology and Laboratory Medicine at the University of British Columbia. This study was undertaken with University of British Columbia research ethics board approval (H18-03050).

Chapter 2 is based on the publication:
Taylor D. Pobran, Lauren M. Forgrave, Yu Zi Zheng, John G.K. Lim, Ian R.A. Mackenzie, and Mari L. DeMarco. Detection and Characterization of TDP-43 in Human Cells and Tissues by Multiple Reaction Monitoring Mass Spectrometry. Clinical Mass Spectrometry. 2019;14: 66-73

For this study, I led the data collection and analysis, and the drafting of the manuscript. Lauren M. Forgrave developed the tissue homogenization method and contributed to manuscript edits. Yu Zi Zheng and John G.K. Lim were involved in early method development. Ian R.A. Mackenzie provided the tissue specimens. Dr. Mari L. DeMarco was the principal investigator and she conceptualized the study and was involved in data interpretation and the writing of the manuscript.

Chapter 3 is based on unpublished works. For this study, I led the data collection and analysis, and the drafting of the study results. Dr. Mari L. DeMarco was the principal investigator and she conceptualized the study and was involved in data interpretation and contributed to the editing of this chapter.

Table of Contents

List of Tables

List of Figures

List of Abbreviations

acetonitrile (ACN)

ammonium hydrogen carbonate (AHC)

amyotrophic lateral sclerosis (ALS)

cerebrospinal fluid (CSF)

coefficient of variation (CV)

collision energy (CE)

declustering potential (DP)

ethylenediaminetetraacetic acid (EDTA)

expected peak area ratio (ePAR)

frontotemporal dementia (FTD)

frontotemporal lobar degeneration (FTLD)

heterogeneous ribonucleoprotein (hnRNP)

horseradish peroxidase (HRP)

human embryonic kidney (HEK)

immunoglobulin G (IgG)

internal standard (IS)

intravenous immunoglobulin G (IVIg)

liquid chromatography tandem mass spectrometry (LC-MS/MS)

lower limit of detection (LLOD)

multiple reaction monitoring (MRM)

n-lauroylsarcosine (sarkosyl)

phosphate-buffered saline (PBS)

post-translational modification (PTM)

recombinant (rec)

RNA recognition motif (RRM)

signal-to-noise ratio (S/N)

sodium dodecyl sulfate polyacrylamide gel electrophoresis (SDS-PAGE)

transactive response DNA-binding protein 43 kDa (TDP-43)

tris-buffered saline (TBS)

tris-ethylenediaminetetraacetic acid (TE)

tosyl phenylalanyl chloromethyl ketone (TPCK)

Acknowledgements

I would like to thank my supervisor Mari DeMarco for giving me the opportunity to work on this project and for helping me develop as a research scientist.

My lab members, Lauren Forgrave, Meng Wang, and David Yang, as well as lab alumni Junyan Shi, Serena Singh, and Amy Nguyen, for their support throughout this project.

My committee chair, Dana Devine, and committee members Joerg Gsponer and Graham Sinclair, for their contribution of time, input, and guidance during my thesis.

My external examiner, Bruce McManus, for his involvement in the critique of my thesis defense.

Chapter 1: Introduction

1.1 The TARDBP Gene

Transactive response (TAR) DNA-binding protein 43 kDa (TDP-43) was first discovered in 1995 as a transcription repressor of the human immunodeficiency virus type 1 genome, where it bound to a regulatory element known as TAR [1]. TDP-43 is encoded by *TARDBP*, a gene that is highly conserved across eukaryotic species including mouse, *Drosophila melanogaster*, and *Caenorhabditis elegans* [2]. Ubiquitously expressed in human tissues, TDP-43 mRNA expression has been found in the heart, brain, testis, ovary, placenta, lung, muscle, kidney, pancreas, and more [1, 3].

1.2 TDP -43 Structure and Function

TDP-43 is a 414 residue, heterogeneous nuclear ribonucleoprotein (hnRNP) that contains a nuclear localization and export signal sequence that enables nucleo-cytoplasmic shuttling (Figure 1) [4]. Like most members of the hnRNP family, TDP-43 contains two central RNA recognition motifs (RRMs) [5] and a glycine-rich region involved in protein-protein interactions [6]. Additionally, this glycine-rich region contains an asparagine- and glutamine-rich prion-like domain, which is thought to contribute to the propensity of TDP-43 to aggregate [7].

While discovered originally as a binder of DNA [1], six years later, TDP-43 was found to modulate alternative splicing of the cystic fibrosis transmembrane conductance regulator RNA [3], a protein that when mutated, is known to cause the fatal genetic disease, cystic fibrosis. In another RNA-binding role, TDP-43 has been described to stabilize human neurofilament light

protein mRNA during recruitment to stress granules, in turn preventing degradation [8]. TDP-43 has also been shown to play a role in microRNA biogenesis, a process essential for neuronal outgrowth [9].

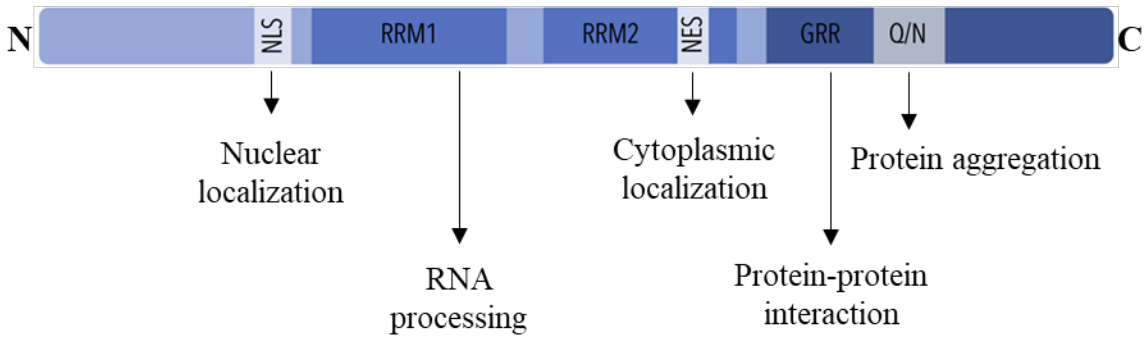

Figure 1: TDP-43 protein domains and cellular functions (NLS: nuclear localization sequence; RRM: RNA recognition motif; NES: nuclear export sequence; GRR: glycine-rich region; Q/N: glutamine- and asparagine-rich region).

1.3 TDP-43 In Neurodegenerative Disease

Frontotemporal dementia (FTD) is a clinically, genetically, and pathologically heterogenous group of diseases that are characterized by progressive neurodegeneration of the frontal and temporal cerebral lobes [10]. FTD is the second most common form of early-onset dementia, after Alzheimer's disease, with the majority of cases occurring before the age of 65 [11]. Recent prevalence estimates of epidemiological studies in Europe and the United Sates range from 3 to 15 per 100,000 adults; these figures may be underestimates as the disease heterogeneity can lead to misdiagnosis, with a definitive diagnosis that can only be made upon autopsy [12].

Amyotrophic lateral sclerosis (ALS), also known as Lou Gehrig's disease, is the most common form of motor neuron disease and is characterized by progressive neurodegeneration in the brain

and spinal cord [13]. In the United States and Europe, there are an estimated 3 to 5 cases per 100,000 adults [14].

Before 2006, the histopathological hallmark of the majority of FTD and ALS cases was the presence of ubiquitin-positive and tau-negative inclusion bodies in central nervous tissue [15-17]. TDP-43 was subsequently discovered to be the main constituent of these inclusions [18, 19]. Thus, the pathology of FTD and ALS associated with TDP-43 inclusions is now defined by immunohistochemical detection of TDP-43 aggregates. In FTD, this pathological finding is termed frontotemporal lobar degeneration with TDP-43 inclusions (FTLD-TDP) [20].

1.4 Detection and Characterization of TDP-43

While the exact role of TDP-43 in the pathogenic mechanism of FTD and ALS remains elusive, post-translational modifications (PTMs) of TDP-43 in FTLD-TDP brain tissue, as well as ALS brain and spinal cord tissue, have been identified. The existence of a range of phosphorylated, ubiquitinated, and truncated forms of TDP-43 in pathological specimens is supported predominantly by western blot analyses and immunohistochemical staining [10, 21-23]. Of these PTMs, truncated TDP-43 isoforms are among the most well-studied, however, much of this work was done *in vitro* and in mouse models. These truncated species of TDP-43 are thought to disrupt the function of normal RNA binding, as well as cellular trafficking, as truncation results in the loss of the nuclear localization signal, and thus disrupts TDP-43 nuclear import and export.

With the majority of TDP-43 detection done by western blot analyses and immunohistochemical staining, characterization of PTMs has relied on epitope-ligand binding methods. Unfortunately,

western blot analysis has revealed that several anti-TDP-43 and secondary anti-IgG antibodies demonstrate high cross-reactivity with human immunoglobulins (e.g., IgG heavy chain at ~ 50 kDa and light chains at ~25 kDa) and albumin (~66 kDa) (Figure 2) [24-26]. Given the importance of the identification of TDP-43 proteolytic fragments (TDP-43 molecules < 43 kDa) and other PTMs that may result in an increase the molecular weight of TDP-43 (e.g., phosphorylation or ubiquitination), there is concern that the lack of specificity of anti-TDP-43 antibodies could be misinterpreted as the presence of TDP-43 PTMs.

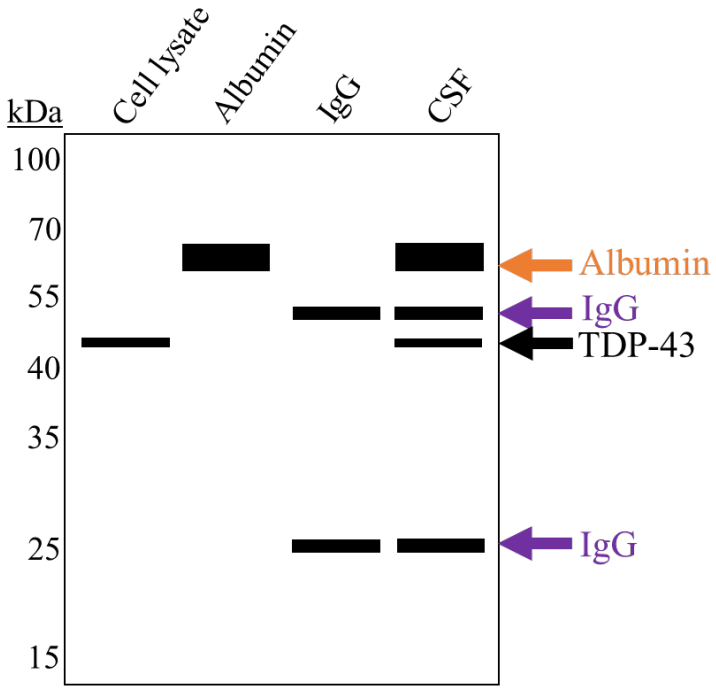

Figure 2: Typical western blot banding observed during detection of TDP-43. Specimens depicted include cell lysate, purified albumin and IgG, and human cerebrospinal fluid (CSF).

1.5 Hypothesis and Aims

We hypothesized that the application of enrichment techniques and detection by mass spectrometry would improve the characterization of TDP-43. The two following aims were set to test the hypothesis:

1. Direct detection of TDP-43 in biological matrices via mass spectrometry
2. Enrichment of TDP-43 from complex human biological matrices

In Aim 1, the goal was to develop a reversed-phase high performance liquid chromatography tandem mass spectrometry (LC-MS/MS) method, using a triple quadrupole mass spectrometer, for the detection of TDP-43, to increase the specificity via detection at the peptide level, rather than relying on the epitope-ligand binding methods. In Aim 2, to improve analytical sensitivity and specificity, the goal was to develop an enrichment protocol compatible with downstream LC-MS/MS analysis. The methodological approaches developed were tested on human cell lines and brain tissue.

Chapter 2: Direct Detection of TDP-43 in Biological Matrices

2.1 Introduction

TDP-43 aggregates are the defining pathology in the majority of cases of FTD and ALS. To better understand the various disease-related modifications (i.e., N-terminal truncation) methods that enable monitoring of changes across the TDP-43 sequence are desirable. Unfortunately, the majority of disease-specific PTMs findings have been generated by immunometric methods, which rely on antigen recognition via short (5-7 residues) epitopes on the protein's surface. It would also be valuable to be able to characterize TDP-43 in a routine manner on common analytical instrumentation. With the development of a method that detects multiple peptides (produced *in vitro*) spanning the TDP-43 sequence, the detection and relative ratios of these TDP-43 peptides could be used as indicators of the presence of PTMs. A TDP-43 peptide signature, based on unmodified peptides, is expected to be altered in the presence of non-uniform PTM of the protein sequence. For example, an increase in the amount of N-terminally truncated TDP-43 *in vivo* is hypothesized to result in a decrease in the number of *in vitro* proteolytic N-terminal peptides observed and the ratio of *in vitro* proteolytic peptides from the N-terminal domain to the central or C-terminal domains.

To address the need for selective and multiplex detection of TDP-43 isoforms from complex biological matrices, we have developed a targeted bottom-up TDP-43 high-performance liquid chromatography tandem mass spectrometry (LC-MS/MS) assay. As proof-of-concept, the method was applied to the detection of TDP-43 from human cell lysate, and brain tissue from an FTLD-TDP case and an unaffected individual.

2.2 Methods

2.2.1 Materials

2.2.1.1 Reagents

The following materials were obtained from the indicated commercial sources: formic acid [399388], N,N,N',N'-tetramethylethylenediamine [T9281], Tween 20 [P1379], phosphate-buffered saline (PBS) [P4417], ammonium persulfate [A3678], ethanol [362808], sodium dodecyl sulfate (SDS) [L3771], sodium chloride (NaCl) [S7653], ethylenediaminetetraacetic acid (EDTA) [E4884], N-lauroylsarcosine (sarkosyl) [61745], urea [U5378], and Dulbecco's modified Eagle's medium [D6429], were obtained from Sigma-Aldrich (Canada). Ammonium hydrogen carbonate (AHC) [A18566], acrylamide/bis-acrylamide solution [J63279], Laemmli SDS sample buffer [J61337], Coomassie brilliant blue G-250 solution [786-497], de-staining solution [786-499], 1.5 mL Protein LoBind tubes [022431081], Roche protease inhibitors [4693159001], acetonitrile (ACN) [BDH83640], tris [0826], CHAPS [0465], bovine serum albumin (BSA) [0332], and tris-buffered saline (TBS) [97063-680] were obtained from VWR (Canada). Nitrocellulose membrane [1620115] and Clarity Max ECL substrate [1705062] were obtained from Bio-Rad. Gibco fetal bovine serum [12483-020], penicillin-streptomycin [15070-063], and molecular weight protein ladder [26616], were obtained from Thermo Fisher Scientific (Canada). Methanol [A456-4] and filter paper [09-802-1A] were obtained from Fisher Scientific. Tosyl phenylalanyl chloromethyl ketone-treated (TPCK) trypsin [LS003744] was obtained from Worthington (USA). Lyophilized recombinant full-length human TDP-43, expressed in *E. coli* with an N-terminal 6*His-tag (referred to, herein, as recTDP-43) [Ag13119] was obtained from ProteinTech (USA). Anti-TDP-43 mouse monoclonal antibody [H00023435-M01] was obtained

from Abnova (Taiwan). Horseradish peroxidase (HRP)-conjugated goat anti-mouse IgG antibody [sc-2005] was obtained from Santa Cruz Biotechnology (USA). The following unlabeled peptides were synthesized by New England Peptide (USA): GISVHISNAEPK, FTEYETQVK, and FGGNPGGFGNQGGFGNSR. C18 tips were obtained from Agilent [5188-5239] and Thermo Fisher [60109-412]. A 1 mL, 26-gauge needle [309597] was obtained from Becton, Dickinson and Company (NJ, USA). HeLa cells [ATCC CCL-2] were obtained from the American Type Culture Collection.

2.2.1.2 Instrumentation

Equipment utilized included: microvolume spectrophotometry (ND-8000, NanoDrop Technologies), centrifugal vacuum (Vacufuge plus, Eppendorf), and a gel imager (G:BOX Chemi XRQ, Syngene). For LC-MS/MS, samples were analyzed using an Aeris Peptide 3.6 μm XB-C18, 50 x 2.0 mm column (Phenomenex, USA) on a Shimadzu LC 20AD LC system coupled to a SCIEX 5500 triple quadrupole mass spectrometer (USA).

2.2.1.3 Human Specimens

This study was undertaken with University of British Columbia research ethics board approval. For the proof-of-concept analysis, frontal lobe brain tissue samples from an individual with immunohistochemistry-confirmed FTLD-TDP type A and from an unaffected individual, were obtained from the Neurodegenerative Brain Biobank at the University of British Columbia. Specimens were collected at autopsy, fresh-frozen, and stored at -70 °C until analysis.

HeLa cells were cultured in Dulbecco's modified Eagle's medium and supplemented with 10 % fetal bovine serum and a penicillin/streptomycin cocktail (100 μg/mL).

2.2.2 Sample Preparation

2.2.2.1 Tissue Homogenization

Human frontal lobe brain tissue (0.2 g) was homogenized manually using a pestle for 2 minutes in 1 mL of tris-EDTA (TE) buffer (10 mM tris-HCL and 1 mM EDTA, pH 7.5, and protease inhibitor cocktail) containing 10 % sucrose, 0.8 M NaCl, and 2 % Tween 20, heated for 30 minutes at 37 °C, and centrifuged at 100,000 x *g* for 30 minutes at 20 °C. The supernatant was collected (Tween-soluble fraction [s1]), and the pellet was homogenized (following the same steps as above) in TE buffer containing 1 % sarkosyl. Again, the supernatant was collected (sarkosyl-soluble fraction [s2]), and the pellet was homogenized in TE buffer containing 1 % CHAPS and centrifuged at 100,000 x *g*. The final supernatant was collected (CHAPS-soluble fraction [s3]), and the resulting insoluble fraction (p) was combined with urea buffer (50 mM tris, pH 8.5, 8M urea and 2 % SDS) and sonicated in 1 second pulses, five times. All fractions were stored at -70 °C until analysis.

2.2.2.2 Cell Lysis

HeLa cells were washed with PBS before the addition of ddH_2O and incubation at 37 °C for 5 minutes. After incubation, the cells were left at room temperature for 5 minutes and then passed through a 26-gauge needle multiple times to rupture remaining intact cells. The resulting lysate was centrifuged at 13,000 x *g* for 15 minutes, at 4 °C. The supernatant was collected, aliquoted,

protein concentration determined by microvolume spectrophotometry, and stored at -70 °C until analysis.

2.2.2.3 Gel Electrophoresis, Western Blot, and In-Gel Digestion

RecTDP-43, HeLa cell lysate, and FTLD-TDP and unaffected homogenate fractions were separated on duplicate 10 % polyacrylamide gels by electrophoresis under denaturing conditions. Proteins were transferred to a nitrocellulose membrane for western blot analysis. The membrane was blocked with 5 % BSA, dissolved in TBS with Tween 20 (0.05 %) (TBS-T), for 1 hour. The membrane was washed 3 times with TBS-T and probed with anti-TDP-43 antibody (1:1,000 in 5 % BSA in TBS-T) overnight at 4 °C. The membrane was then washed again and incubated in HRP-conjugated anti-mouse (1:10,000 in 5 % BSA in TBS-T) for 1 hour at room temperature. The blot was washed for a final time before being imaged using ECL substrate.

Prior to in-gel digestion, total protein was stained for one hour in Coomassie dye and then de-stained overnight prior to imaging. Bands were excised from the gel and placed into separate tubes. To prepare gel pieces for digestion, sequential incubations were performed at room temperature for 20 minutes in each of the following solutions: 50 mM AHC; 50 % 25 mM AHC, 50 % ACN; and 100 % ACN. Gel pieces were then rehydrated in 50 mM AHC with 5 µg of TPCK-trypsin and incubated overnight at 37 °C. The digestion was halted by adding 1 % formic acid to a final concentration of 0.1 %. The supernatant was removed and saved for analysis. Remaining gel pieces were further extracted with 100 uL of 50 % ACN and 0.1 % formic acid in water and incubated at room temperature for 20 minutes. A final extraction using 100 % ACN

was performed. All extractions were combined, and the resulting mixture dried by vacuum centrifugation.

Samples were reconstituted in 0.5 % formic acid and desalted using C18 tips (Agilent tips for HeLa cells and Thermo Fisher tips for brain tissue) according to the manufacturer's protocol, with the substitution of formic acid for trifluoroacetic acid.

2.2.3 Proteotypic Peptide Selection and MRM Method Development

Tryptic peptides spanning TDP-43 residues 56-79, 103-114, 152-160, 182-189, 252-263, and 276-293 (referred to as TDP_{56-79}, $TDP_{103-114}$ $TDP_{152-160}$, $TDP_{182-189}$, $TDP_{252-263}$, and $TDP_{276-293}$, respectively), were selected based on previously developed criteria and subsequent empirical evaluation of recTDP-43. The recTDP-43 was denatured at 95 °C for 10 minutes and incubated with TPCK-trypsin for 4 hours at 37 °C, and halted by the addition of 1 % formic acid – following our group's previously developed approach to the design of digestion workflows suitable for clinical laboratory implementation [27]. For each of the six TDP peptides, the most abundant precursor ion and three product ions were selected for monitoring.

2.2.4 LC-MS/MS Optimization

MS parameters were optimized using both tryptic digests of recTDP-43 in buffer and synthetic TDP-43 peptides. Collision energy (CE) and declustering potential (DP) were optimized for each MRM. Mobile phases A and B consisted of 0.1 % formic acid in water and 0.1 % formic acid in ACN, respectively. A flow rate of 0.25 mL/min and column temperature of 45 °C was used with

the following gradient: 5 % B from 0 to 1 minute, 5 – 95 % B from 1 to 7.5 minutes, 95 % B from 7.5 to 8.5 minutes, and 5 % B from 8.5 to 12 minutes for re-equilibration.

2.2.5 Figures of Merit

The criteria for the lower limit of detection (LLOD) was a signal-to-noise (S/N) ratio ≥ 3 for the quantifier ion and transition peak area ratios (PARs) within 15 % of the standard ratios for the qualifier ions. S/N was calculated as peak-to-peak where the maximal noise peak was considered within a 0.2-minute retention time window of the signal peak.

Linearity was assessed by serially diluting a 1 μg/mL recTDP-43 tryptic digest solution, halving the concentration in 8 dilutions from 500 to 3.91 ng/mL using 50 mM AHC.

2.2.6 Data Analysis

The observed m/z of peptide precursor and product ions were verified using Skyline [28]. Each peptide sequence was assessed for its uniqueness for TDP-43 within the human proteome by protein BLAST search and the sequence explored for variants and potential PTMs including ubiquitination, phosphorylation, sumoylation, acetylation, glycosylation, and truncation using the Universal Protein Resource (Uniprot). LC-MS/MS data was analyzed using Analyst software (SCIEX v.1.6) and linear regressions performed using cp-R software [29].

2.3 Results

2.3.1 TDP-43 Characterization, Peptide Selection, and MRM Development

The six peptides selected by *in silico* digestion were determined to be unique for TDP-43 within the human proteome (Figure 3). Exploration of potential PTM sites and variants relevant to the peptide sequences monitored revealed reports of sumoylation of K_{79} and K_{263} [30], phosphorylation of S_{183} and S_{292} [31], methylation of R_{293} [32], a $P_{112}H$ variant in a case of FTLD-TDP [33], a $K_{263}E$ variant in a case of FTLD-TDP with supranuclear gaze palsy and chorea, a $G_{287}S$ variant in a case of sporadic ALS, and $G_{290}A$ and $S_{292}N$ variants in cases of familial ALS [10].

An MRM method was developed that monitored the six TDP-43 proteotypic peptides (Figure 4). By empirical evaluation, retention times were confirmed and three precursor to product ion transitions per peptide were selected for monitoring (Figure 5). Optimized MRM parameters are found in Table 1.

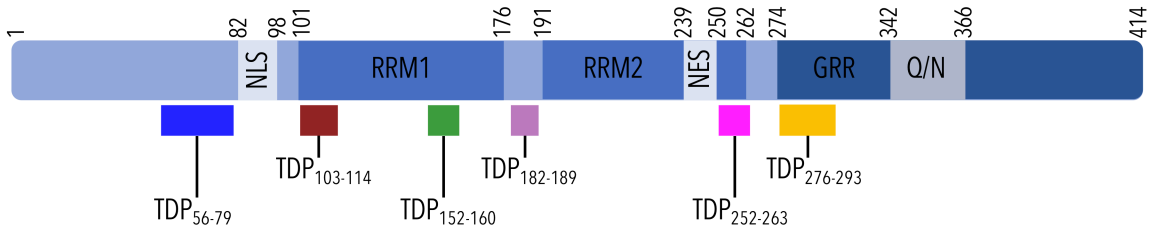

Figure 3: TDP-43 protein sequence and the six proteotypic peptides monitored in the MRM LC-MS/MS method.

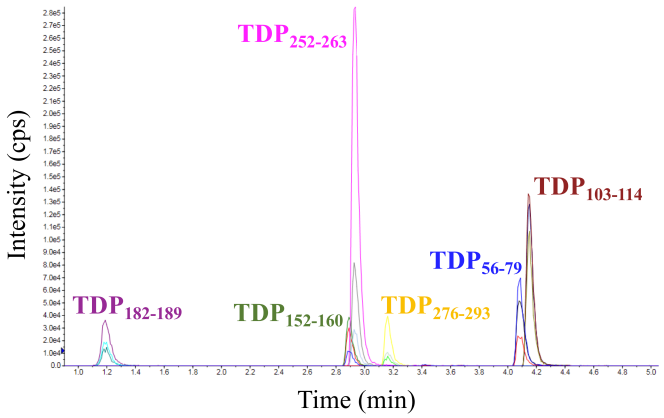

Figure 4: Representative chromatogram of the TDP-43 6-plex MRM assay.

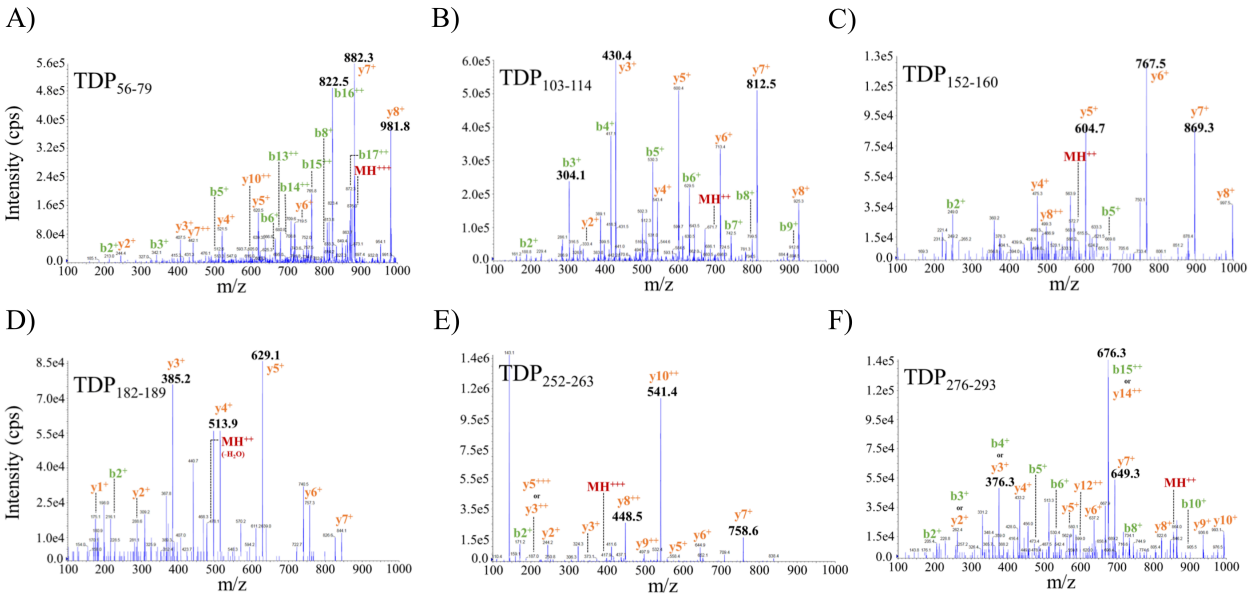

Figure 5: Product ion scans of recTDP-43 tryptic peptides pre-optimization.

Table 1: Optimized MRM parameters for proteotypic TDP-43 peptides.

Peptide	Q1 ion (m/z)	Q1 charge state	Q3 ion (m/z)[a]	Fragment ion	DP (V)	CE (V)
TDP_{56-79}	875.8	3+	822.5	b_{16}	100	30
			882.3	y_7	100	30
			981.8	y_8	100	30
$TDP_{103-114}$	671.6	2+	430.4	y_3	80	40
			304.1	b_3	80	40
			812.5	y_7	80	30
$TDP_{152-160}$	572.8	2+	869.3	y_7	40	26
			767.5	y_6	40	30
			604.7	y_5	40	30
$TDP_{182-189}$	486.7	2+	513.9	y_4	80	28
			629.1	y_5	80	28
			385.2	y_3	80	28
$TDP_{252-263}$	417.9	3+	541.4	y_{10}	80	23
			448.5	y_8	80	22
			758.6	y_7	80	20
$TDP_{276-293}$	863.9	2+	676.3	y_{14}	60	40
			376.3	y_3	60	40
			694.3	y_7	60	42

[a] Listed in order of the quantifier ion first, followed by the two qualifier ions.

2.3.2 Sensitivity and Linearity

Based on structural characterization and intensity in the LC-MS/MS, $TDP_{252-263}$ was selected for assessment of assay sensitivity and linearity. Structurally, $TDP_{252-263}$ is situated at the immediate C-terminal end of RRM2. Sumoylation of K_{263} at the C-terminal end of $TDP_{252-263}$ has been reported; however, this is from a single, untargeted study analyzing the human sumoylation

proteome with no confirmatory analysis performed [30]. A $K_{263}E$ variant has been reported in a single case of FTLD-TDP with supranuclear gaze palsy and chorea [10].

By analysis of a dilution series of trypsin-digested recTDP-43 in 50 mM AHC, the lower limit of detection for TDP-43 was determined to be 3.91 ng/mL (Table 2). LC-MS/MS analysis of the $TDP_{252-263}$ MRM was linear over the range of 3.91 ng/mL to 500 ng/mL based on least squares regression analysis of the dilution series; $R^2 = 0.9996$ (Figure 6).

Table 2: Comparison of recTDP-43 dilution series against detection criteria of S/N ≥ 3 and PAR within ± 15% of expected (ePAR) for $TDP_{252-263}$.

TDP-43 (ng/mL)	S/N	% from ePAR[a]	
		Qualifier-1 (448.5 m/z)	Qualifier-2 (758.6 m/z)
500	> 100	-4	0
250	> 100	-4	0
125	> 100	-11	0
62.5	> 100	-14	0
31.25	> 100	-4	-11
15.63	> 100	-11	-11
7.81	> 73	-11	-11
3.91	> 35	-11	-11
1.95[b]	> 22	-14	-56
0.98[b]	> 16	-4	-22
0.49[b]	8	+36	-22
0.24[b]	3	-25	+11

[a] Deviation from the expected peak area ratio for recTDP-43

[b] Failed detection criteria

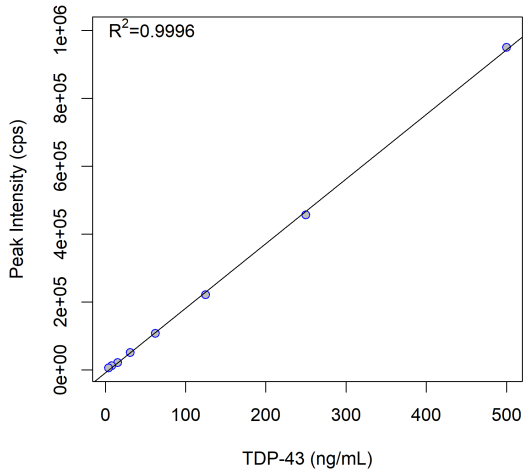

Figure 6: Linearity of the response of $TDP_{252-263}$.

2.3.3 Detection of Endogenous TDP-43 in HeLa Cell Lysate

TDP-43 western blot analysis of HeLa cell lysate and recTDP-43 (with an N-terminal HIS-tag and a theoretical molecular mass of 48,284 Da) yielded bands in the expected molecular weight regions of 43 kDa and 49 kDa, respectively (Figure 7).

Gel regions where TDP-43 was detected by western blot were excised, digested, and analyzed by LC-MS/MS, which confirmed the presence of TDP-43. For HeLa cells, five TDP-43 tryptic peptides were observed, of which four (TDP_{56-79}, $TDP_{103-114}$, $TDP_{152-160}$, and $TDP_{252-263}$) satisfied the assay detection acceptance criteria (Table 3).

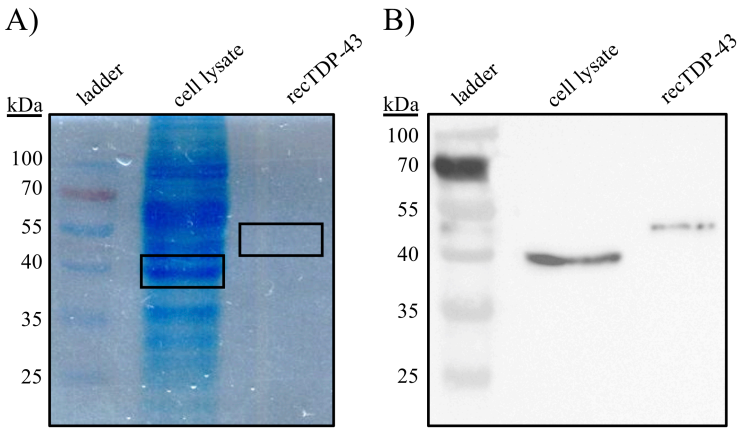

Figure 7**:** (A) SDS-PAGE and (B) TDP-43 western blot analysis of HeLa cell lysate and recTDP-43. Boxes indicate gel excisions subjected to in-gel digest and LC-MS/MS analysis.

Table 3: LC-MS/MS analysis of the in-gel digestion of HeLa cell lysate TDP-43 band.

Peptide	Quantifier ion S/N	Qualifier ions (m/z)	% from ePAR[a]
TDP_{56-79}	40	882.3	-15
		981.8	+15
$TDP_{103-114}$	49	304.1	+7
		812.3	+1
$TDP_{152-160}$	18	767.4	-11
		604.3	-13
$TDP_{252-263}$	37	448.2	-11
		758.4	-15
$TDP_{276-293}$	22	376.3	+7
		694.3	-24[b]

[a] Deviation from the expected peak area ratio for recTDP-43

[b] Failed acceptance criteria of ePAR within ± 15%

2.3.4 Detection of Endogenous TDP-43 in Human Brain Tissue

Human brain tissue from an unaffected individual and an individual with FTLD-TDP type A was homogenized and fractionated, by increasing the strength of the detergent. The three soluble fractions (s1-s3) and one insoluble fraction (p) were analyzed by western blot and LC-MS/MS after in-gel digestion. Via western blot, TDP-43 was observed in all fractions for both specimens, except fraction s3 of the unaffected specimen (Figure 8). Gel regions where TDP-43 was observed by western blot (around 43 kDa) were excised and subjected to in-gel digestion and LC-MS/MS analysis. In all western blot-positive gel pieces, LC-MS/MS identified multiple TDP-43 peptides. In these samples, LC-MS/MS identified four (unaffected s2 and FTLD-TDP s1) or five (unaffected s1 and p; FTLD-TDP s2, s3, and p) TDP-43 proteotypic peptides; and at least one peptide for each fraction met the pre-specified detection criteria (Table 4). Additionally, two TDP-43 peptides (TDP_{56-79} and $TDP_{103-114}$, with the latter meeting the pre-

defined detection criteria) were identified in the gel section from the unaffected s3 fraction, which was western blot-negative for TDP-43 (Table 4).

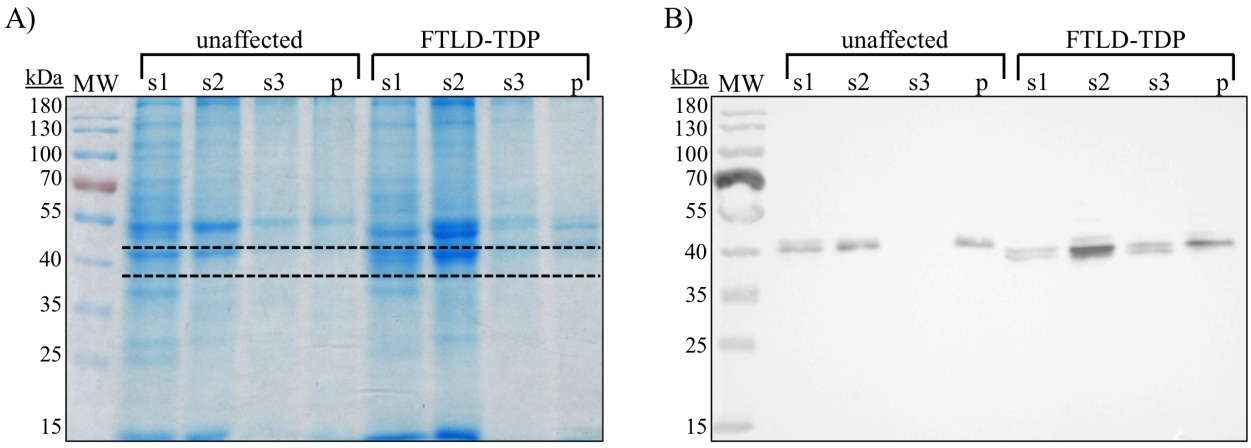

Figure 8: (A) SDS-PAGE and (B) western blot analysis of unaffected and FTLD-TDP type A human brain tissue homogenate soluble fractions (s) and insoluble fraction (p) (dashed line: gel region excised for in-gel digestion and LC-MS/MS analysis).

Table 4: LC-MS/MS detection of TDP-43 in the insoluble fractions from the unaffected and FTLD-TDP type A frontal lobe tissue specimens.

Peptide	Q3 ion (m/z)	Unaffected tissue		FTLD-TDP tissue	
		Quantifier ion S/N	% from ePAR[a]	Quantifier ion S/N	% from ePAR[a]
TDP_{56-79}	882.3	7	-7	4	-5
	981.8		+3		+22[b]
$TDP_{103-114}$	304.1	23	-12	31	+4
	812.3		-16[b]		-15
$TDP_{152-160}$	767.4	6	+17[b]	9	+22[b]
	604.3		+31[b]		+9
$TDP_{252-263}$	448.2	32	+14	22	+11
	758.4		0		+11
$TDP_{276-293}$	376.3	29	+40[b]	14	+13
	694.3		+24[b]		+22[b]

[a] Deviation from the expected peak area ratio for recTDP-43

[b] Failed acceptance criteria of ePAR within ± 15%

2.4 Discussion

While TDP-43 has been identified as the defining pathological protein in the majority of FTD and ALS cases, there remain gaps in our knowledge about the structure of TDP-43 in these disease states. As such, there is great interest in detecting, characterizing and quantifying TDP-43 and its disease-related PTMs. To date, methods to study TDP-43 have largely relied on

ligand-binding methods, which lack specificity for TDP-43 and the resolution to characterize sequence structure. To overcome this obstacle, we developed a multiplex LC-MS/MS method selective for proteotypic peptides of TDP-43. By shifting the detection of TDP-43 to the proteolytic peptide level, higher sequence level information can be obtained. This information can in turn be utilized to create TDP-43 peptide signatures (relative proteolytic peptides amounts) characteristic of TDP-43 proteinopathies compared to controls.

To assess detection of natively-folded endogenous TDP-43 in a complex biological sample, the LC-MS/MS method was applied to detection of endogenous TDP-43 in a human cell line. While analysis of recTDP-43 is helpful for method development, it is not an ideal surrogate for the natively structured protein. The recTDP-43 used had a non-cleavable 6*HIS-tag on the N-terminus and, based on several lots purchased and analyzed by western blot, was of varying purity; moreover, recTDP-43 is known to readily form aggregates in physiological buffers [34], which is not representative of natively folded endogenous TDP-43. As such, recTDP-43 is helpful in early method development, but ultimately endogenous TDP-43 from human sources should be tested.

Human cell lines are one such native source, and are particularly relevant due to the prevalence of FTD and ALS research conducted using human cell lines. While animal models are commonly studied in related neurodegenerative disorders, such as Alzheimer's disease, there are challenges in creating animal models of TDP-43 pathology that fully recapitulate the findings in humans. To create an FTLD-TDP/ALS animal model, human TDP-43 must be transgenically overexpressed or knocked-in. While these two models can present with mild to moderate

disease-associated phenotypes, the predominant pathological hallmark of the disease – neuronal cytoplasmic TDP-43 inclusions – are not always present [35]. Transgenic mice expressing similar amounts of human TDP-43 compared to humans develop age-dependent neurological phenotypes, but without neuronal loss, paralysis or reduced lifespan [35]. The use of human cell lines for studying TDP-43 pathogenesis has, thus, been an important focus of FTD/ALS research [36-38].

The LC-MS/MS method applied to the characterization of HeLa cells successfully detected proteolytic peptides from endogenous TDP-43. Detection post-in-gel-digest, yielded observation of five TDP-43 peptides of which TDP_{56-79}, $TDP_{103-114}$, $TDP_{152-160}$, and $TDP_{252-263}$ satisfied the detection acceptance criteria. The LC-MS/MS detected peptides had wide sequence representation covering multiple structural domains of TDP-43, including pathologically relevant sites. TDP-43 regions detected include the N-terminus and RNA binding domains, RRM1 and RRM2, which encompass the nuclear localization and export signal sequences. Detection of peptides from the RNA binding domains (residues 101-262) represent the functional domain of TDP-43 [5]. Pathologically relevant sites covered include disease-suspected 35 kDa and 25 kDa caspase cleavage products of TDP-43, that is, TDP-35 and TDP-25 spanning residues 90–414 and 220-414, respectively [39]. In cell lines, cleavage of TDP-43 by caspase 3 into TDP-35 and TDP-25 fragments, leads to redistribution of nuclear TDP-43 into the cytoplasm [39, 40] and can generate aggregation-prone fragments and form cytoplasmic toxic inclusion bodies [41]. While N-terminal and RNA-binding domains were detected, two peptides did not meet the detection criteria, including the one from the C-terminal domain. $TDP_{182-189}$ was not observed, whereas $TDP_{276-293}$ was observed, but failed one of the detection threshold criteria (i.e., a qualifier ion

ratio). Peptides both N-terminal and C-terminal to $TDP_{182-189}$ were detected, which along with relative signal intensities from recTDP-43, suggest inadequate sensitivity for these two peptides due to pre-analytical (e.g., proteolytic cleavage efficiency) and/or analytical factors (e.g., ionization efficiency). Notably, saturation of the C18 tips was observed in the analysis of the HeLa cell lysate (data not shown); this presents an opportunity for future improvements in sensitivity for all monitored tryptic peptides. As a result of this finding, C18 tips with a greater binding capacity were used for analysis of the brain tissue homogenates.

Common contemporary approaches for characterizing TDP-43 structure in brain tissue include immunohistochemical staining and western blot analyses, both of which are ligand binding methods dependent on antibody-antigen interactions. While this methodology has been valuable in the characterization of TDP-43 in disease, it has limited multiplexing capabilities, relies on indirect detection (resulting in a lack of specificity) and provides low-resolution structural information. The availability of a higher resolution method that directly detects the measurand of interest, e.g., MRM LC-MS/MS, would be helpful in routine characterization of tissues, and complement information obtained from immunometric approaches. As proof-of-concept, the ability of the TDP-43 MRM LC-MS/MS assay to detect endogenous TDP-43 in human brain tissue (immunohistochemical-confirmed FTLD-TDP type A and an unaffected control) was assessed.

In general, the low relative abundance of TDP-43 in complex matrices such as brain tissue (particularly the soluble fractions, which had a high non-TDP-43 protein content), presents a challenge for detection. With greater analytical sensitivity desired, the use of larger resin

volumes for desalting and/or additional enrichment strategies, can be applied to further improve the sequence resolution by LC-MS/MS. Further enrichment may also result in sufficient purification of TDP-43 isoforms to enable alternate mass spectrometric approaches, such as top-down analysis. The current selective detection of TDP-43 by MRM LC-MS/MS and sequence coverage achieved for cell lysate and human tissue support the application of this targeted TDP-43 LC-MS/MS assay for routine characterization of FTLD-TDP and ALS pathological tissues, which, with ongoing method development, has the potential to provide even higher sequence resolution to aid in our understanding of structural modifications of TDP-43 associated with neurodegenerative disorders.

2.5 Conclusion

A targeted multiplex mass spectrometric method for the detection and characterization of TDP-43 was developed. The method enabled detection of TDP-43 in complex biological matrices, including human cell lines and human brain tissue specimens, and provides the opportunity for characterization of pathological forms of TDP-43 at higher resolution compared to ligand binding methods.

Chapter 3: Enrichment of TDP-43

3.1 Introduction

In addition to the limited analytical tools available, detailed analysis of TDP-43 in matrices such as blood, brain tissue homogenate, and cell lines is hindered by the complexity of the matrix under investigation and the relatively low abundance of TDP-43. To decrease background interference and improve sensitivity, enrichment of TDP-43 is an option. Immunoenrichment is a commonly used enrichment strategy prior to mass spectrometric analysis, as well as other types of analyses [42]. While antibodies are widely used from research to clinical settings, antibody specificity is an issue [43]. Specific to currently available anti-TDP-43 antibodies, cross-reactivity with albumin and IgG between has been documented [24-26]. This cross-reactivity with highly abundant proteins in human biofluids poses a challenge for accurate and selective detection of TDP-43.

Aptamers, small single-stranded DNA or RNA oligonucleotides (roughly 15 – 50 nucleotides in length) as well as short peptides, are becoming increasingly popular in the field of medicine for diagnostics and therapeutics [44-46]. They are similar to antibodies, by which they can bind target molecules with high affinity and specificity, and can also be attached with various functional groups (i.e., biotin) for downstream applications [47]. Advantages of aptamers include their small size (< 20 kDa), their stability, and being amenable to chemical modification as well as being cost effective to generate *in vitro* [44, 48].

With the goal of utilizing a non-antibody based approach for analyte enrichment, we developed an RNA aptamer enrichment workflow followed by mass spectrometric analysis. The aptamer was selected based on documented high binding affinity for TDP-43 (K_d = 5.3 nM) [49]. The assay was subsequently tested on human cell lysates and human brain tissue for detection, quantitation and characterization of endogenous TDP-43.

3.2 Materials and Methods

3.2.1 Materials

The following materials were obtained from the indicated commercial sources: formic acid [399388], N,N,N',N'-tetramethylethylenediamine [T9281], Tween 20 [P1379], phosphate-buffered saline (PBS) [P4417], ammonium persulfate [A3678], ethanol [362808], sodium dodecyl sulfate (SDS) [L3771], sodium chloride (NaCl) [S7653], ethylenediaminetetraacetic acid (EDTA) [E4884], N-lauroylsarcosine (sarkosyl) [61745], urea [U5378], Dulbecco's modified Eagle's medium [D6429], magnesium chloride ($MgCl_2$) [M8266], and anti-TDP-43 rabbit polyclonal antibody [T1580] were obtained from Sigma-Aldrich (Canada). Ammonium hydrogen carbonate (AHC) [A18566], acrylamide/bis-acrylamide solution [J63279], Laemmli SDS sample buffer [J61337], Coomassie brilliant blue G-250 solution [786-497], de-staining solution [786-499], 1.5 mL Protein LoBind tubes [022431081], Roche protease inhibitors [4693159001], acetonitrile (ACN) [BDH83640], tris [0826], CHAPS [0465], bovine serum albumin (BSA) [0332], acetic acid [36289], and tris-buffered saline (TBS) [97063-680] were obtained from VWR (Canada). Nitrocellulose membrane [1620115] and Clarity Max ECL substrate [1705062] were obtained from Bio-Rad. Gibco fetal bovine serum [12483-020], penicillin-streptomycin [15070-063], molecular weight protein ladder [26616], antibody

biotinylation kit [90407], and streptavidin magnetic beads [88816] were obtained from Thermo Fisher Scientific (Canada). Methanol [A456-4] and filter paper [09-802-1A] were obtained from Fisher Scientific. Tosyl phenylalanyl chloromethyl ketone-treated (TPCK) trypsin [LS003744] was obtained from Worthington (USA). Lyophilized recombinant full-length human TDP-43, expressed in *E. coli* with an N-terminal 6*His-tag [Ag13119] was obtained from ProteinTech (USA). Anti-TDP-43 mouse monoclonal antibody [H00023435-M01] was obtained from Abnova (Taiwan). Horseradish peroxidase (HRP)-conjugated goat anti-mouse IgG antibody [sc-2005] was obtained from Santa Cruz Biotechnology (USA). Stable isotope ^{13}C- and ^{15}N-labeled lysine peptide GISVHISNAEPK and the following unlabeled peptides were synthesized by New England Peptide (USA): GISVHISNAEPK, FTEYETQVK, and FGGNPGGFGNQGGFGNSR. C18 tips were obtained from Agilent [5188-5239] and Thermo Fisher [60109-412]. A 1 mL, 26-gauge needle [309597] was obtained from Becton, Dickinson and Company (NJ, USA). HeLa cells [ATCC CCL-2] were obtained from the American Type Culture Collection. Recombinant RNase inhibitor [M0307] was obtained from New England Biolabs (USA). The following RNA oligonucleotide, with the addition of a 3' biotin molecule linked via a tetraethylene glycol spacer arm, was synthesized by Integrated DNA Technologies (USA): GAGAGAGCGCGUGUGUGUGUGGUGGUGCAUAA.

3.2.2 Human Specimens

This study was undertaken with University of British Columbia research ethics board approval. For the proof-of-concept analysis, frontal lobe brain tissue samples from an individual with immunohistochemistry-confirmed FTLD-TDP type A and from an unaffected individual, were

obtained from the Neurodegenerative Brain Biobank at the University of British Columbia. Specimens were collected at autopsy, fresh-frozen, and stored at -70 °C until analysis.

Human plasma, CSF, and IVIg were obtained from the clinical laboratory at St. Paul's hospital, Vancouver, British Columbia.

HeLa cells were cultured in Dulbecco's modified Eagle's medium and supplemented with 10 % fetal bovine serum and a penicillin/streptomycin cocktail (100 μg/ml). HEK-293 cell pellets were received from Dr. Emanuele Buratti at the International Centre for Genetic Engineering and Biotechnology (Trieste, Italy).

3.2.3 Tissue Homogenization and Cell Lysis

Protocols for tissue homogenization are found in chapter 2.

3.2.4 Immunoenrichment

Anti-TDP-43 rabbit polyclonal antibody was biotinylated following the manufacturer's protocol. Ten micrograms of biotinylated antibody was combined with the sample of analysis containing TDP-43 and incubated overnight at 4°C. The antibody/TDP-43 mixture was then added to pre-washed streptavidin-coated magnetic beads and incubated for one hour at room temperature. Captured TDP-43 was eluted by incubating the bound beads in SDS sample buffer and boiling for 5 minutes at 95°C.

3.2.5 Aptamer Enrichment

Pre-washed streptavidin-coated magnetic beads were incubated with biotinylated RNA for 30 minutes at room temperature. The RNA-bound beads were then incubated in the sample of analysis containing TDP-43, binding buffer (10 mM tris (pH 8.0), 10 mM NaCl, and 2 mM $MgCl_2$), and RNase inhibitor, for 1 hour at 4°C. Captured TDP-43 was either eluted by incubating the bound beads in SDS sample buffer and boiling for 5 minutes at 95°C (western blot analysis), or incubating in 5% acetic acid for 5 minutes at room temperature with mixing (mass spectrometric analysis) (Figure 9).

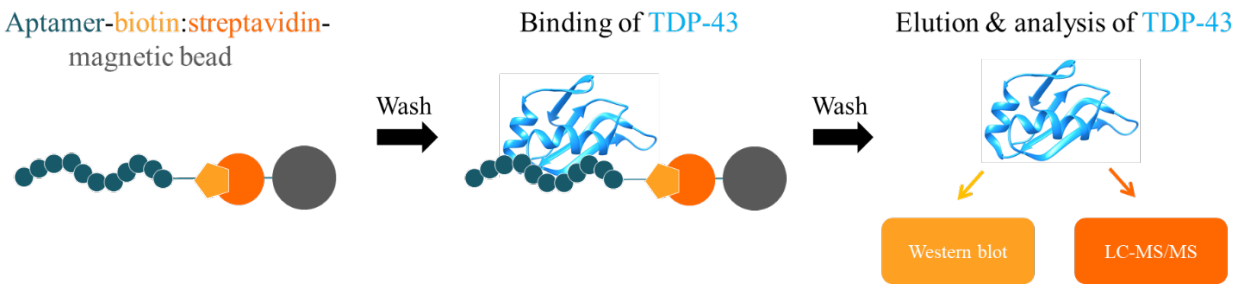

Figure 9: TDP-43 enrichment using an RNA aptamer.

3.2.6 Gel Electrophoresis and Western-Blotting

Samples for electrophoretic gel analysis were separated on a 10% polyacrylamide gel by SDS-PAGE and transferred onto nitrocellulose membrane. The membrane was blocked with 5% dried skimmed milk, dissolved in tris-buffered saline with Tween 20 (0.05%) (TBS-T), for 1 hour. The membrane was then probed with anti-TDP-43 mouse monoclonal antibody at 1:1,000 in 5% BSA / TBS-T, overnight at 4°C. The membrane was washed 3 times with TBS-T and incubated in HRP-conjugated goat anti-mouse at 1:10,000 in 5% BSA / TBS-T, for 1 hour at room

temperature. The blot was then washed 3 times with TBS-T and imaged using Clarity Max Western ECL substrate.

3.2.7 LC-MS/MS Sample Preparation, Internal Standard, Calibration and Analysis

The aptamer-enriched eluates for mass spectrometric analysis were dried-down in by vacuum centrifugation and resuspended in 20 µl of 50 mM AHC. Samples were then denatured at 95°C for 10 minutes and subjected to digestion using TPCK-treated trypsin, for 4 hours at 37°C. The digest reaction was halted by adding 1% formic acid to a final concentration of 0.1%. Calibration was performed by spiking IS to a concentration of 1 ng/mL, to each sample, immediately prior to mass spectrometry analysis. Stable isotope ^{13}C- and ^{15}N-labeled lysine peptide $TDP_{252-263}$ was used as a single point internal calibrator and internal standard (IS). The lyophilized vial was solubilized with deionized water, where the stock and working solutions were then aliquoted and stored at -80 °C. Wild-type HEK cell lysate was used for the method validation experiments and as the quality control.

Samples were analyzed using our previously developed mass spectrometry MRM method, described in Chapter 2, for the detection of TDP-43 (Figure 4) [50], following the previously described parameters, with the substitution of an alternate LC gradient: 1% B from 0 to 1 minute, 1 - 10% B from 1 to 2 minutes, 10 - 13% B from 2 to 4 minutes, 13 - 23% B from 4 to 4.5 minutes, 23 - 35% B from 4.5 to 7 minutes, 35 - 99% B from 7 to 7.1 minutes, 99% B from 7.1 to 8.1 minutes, and 1% B from 8.1 to 10 minutes for re-equilibration.

3.2.8 Method Validation

CLSI guideline C62-A was used as a guide for the method validation experiments [51]. Precision studies were performed by doing triplicate measurements of the quality control, repeated on three different days. Imprecision was expressed as % CV, where the acceptance criteria was set to ≤ 20%. The criteria set for lower limit of the measuring interval (LLMI) was a S/N ≥ 10, in addition to the % CV acceptance criteria. Linearity was determined by performing a mixing experiment. A low pool (1/10 dilution) and high pool (undiluted) of the control were mixed at 4:0, 3:1, 2:2, 1:3, and 0:4, and prepared in duplicate. Ion suppression and enhancement was assessed by performing a post-column infusion experiment. Relevant matrices (described below) were injected to the liquid chromatography stream while a 20 ng/mL solution of the IS was continuously infused into the flow at the mass spectrometer source, at a rate of 7 µL/min, via a T-union. Matrices tested for ion suppression/enhancement included 0.1% formic acid, digestion buffer, and both HeLa and HEK cell lysates.

3.2.9 Data Analysis

LC-MS/MS data was analyzed using Analyst software (SCIEX v.1.6) and linear regressions were performed using cp-R software [29].

3.3 Results

3.3.1 Anti-TDP-43 Antibody Cross-Reactivity

To observe the effect of cross-reactivity displayed by anti-TDP-43 antibodies, neat samples of human cell lysate expressing endogenous TDP-43 (positive control), CSF, plasma, and pooled intravenous IgG (IVIg) (negative control), were subjected to western blot analysis (Figure 10).

While a single dense TDP-43 band at ~43 kDa was observed in the cell lysate, faint banding at ~50 kDa was observed in the negative control lane containing only human IgG, consistent with cross-reactivity to IgG heavy chain. An additional faint band > 60 kDa in the plasma lane is also seen, consistent with the migration pattern of albumin.

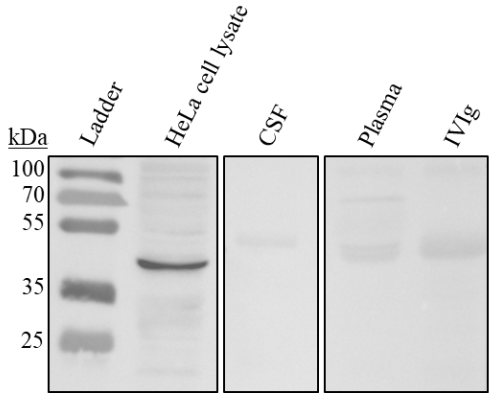

Figure 10: Western blot detection of TDP-43 with a C-terminal specific antibody. Specimens analyzed included HeLa cell lysate, human cerebrospinal fluid (CSF) and plasma, and intravenous IgG (IVIg).

3.3.2 Western Blot Detection of Enriched TDP-43 Using an RNA Aptamer

To visually assess the efficiency of TDP-43 enrichment using the RNA aptamer, TDP-43 western blots of the fractions generated during the enrichment protocol from HeLa cell lysate were performed (Figure 11). A single TDP-43 band was detected in the eluate upon western blot analysis. Total protein stain of the aptamer eluate supported successful TDP-43 enrichment by the lack of protein staining compared to the supernatant.

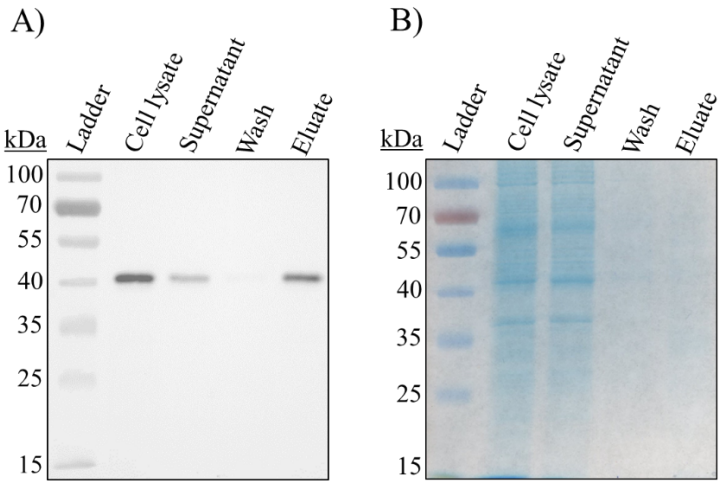

Figure 11: (A) SDS-PAGE and (B) western blot analysis of the aptamer enrichment of endogenous TDP-43 from HeLa cell lysate.

A comparison between aptamer enrichment and immunoenrichment was also performed (Figure 12). Aptamer enrichment of both recTDP-43 and endogenous TDP-43 from HeLa cell lysate yielded a single dense band at ~43 kDa (Figure 12A), while immunoenrichment yielded multiple bands (Figure 12B). The substrates (biotinylated antibody) used for immunoprecipitation contributed to antibody cross-reactivity, whereby leaching of IgG heavy and light chains occurred during elution (data not shown).

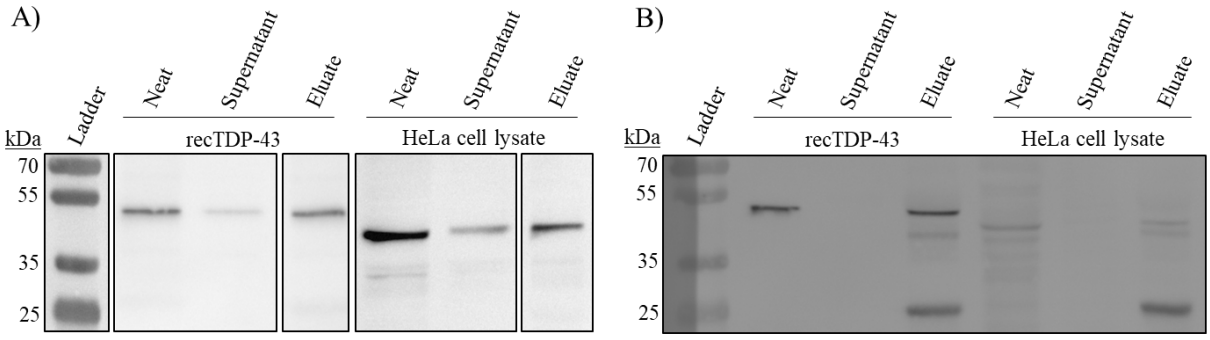

Figure 12: Western blot analysis of (A) aptamer enrichment and (B) immunoenrichment of recTDP-43 and endogenous TDP-43 from human cell lysate.

3.3.3 Figures of Merit for TDP-43 Quantification via Aptamer Enrichment and LC-MS/MS Analysis

With successful aptamer enrichment of TDP-43 supported by western blot and total protein stain analyses, validation of a quantitative LC-MS/MS method for TDP-43 was performed. Within-run, between-run, and total precision CVs were 8.8%, 13.1%, and 15.6%, respectively, with a measured TDP-43 mean of 1.10 ng/mL. The assay was linear over the range of 0.19-2.18 ng/mL, $R^2 = 0.9657$ (Figure 13). Post-column infusion experiments showed no significant ion suppression or enhancement at the retention time of $TDP_{252\text{-}263}$ (3.95 minutes) (Figure 14).

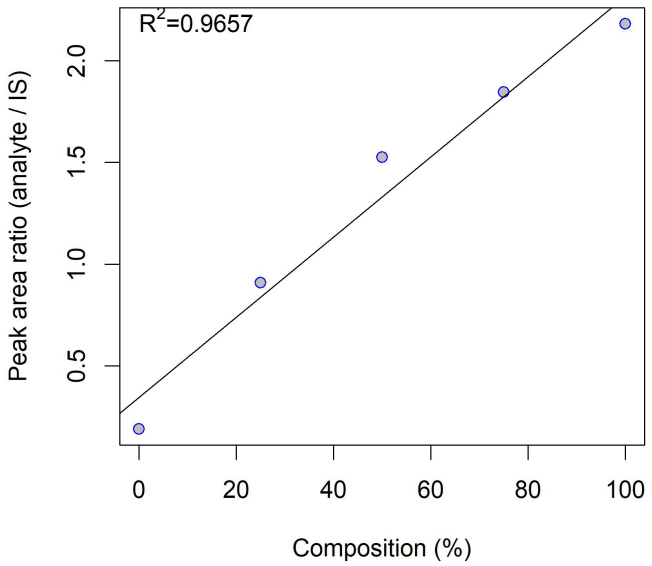

Figure 13: Linearity. Peak area ratio of aptamer-enriched endogenous TDP-43 to IS from increasing high pool composition of HEK cell lysate.

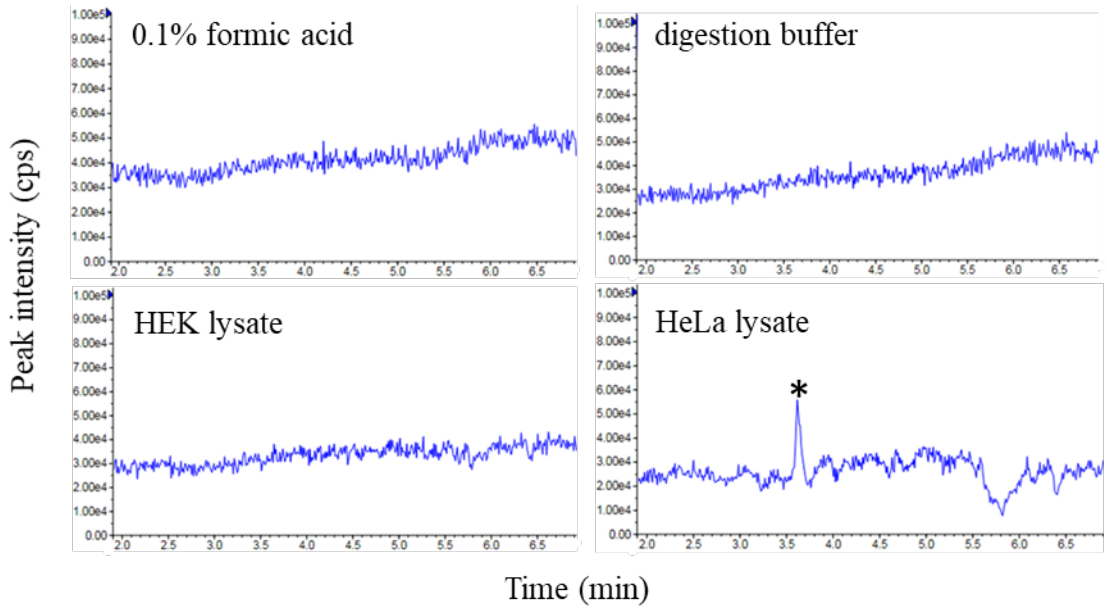

Figure 14: No ion suppression or enhancement is observed during continuous post-column infusion at the retention time of peptide $TDP_{252-263}$, expected at ~3.95 minutes (* denotes peak at 3.62 minutes that was separated chromatographically from the IS peak).

3.3.4 Mass Spectrometric Detection and Quantitation of Aptamer-Enriched TDP-43

Assessment of aptamer enrichment coupled to LC-MS/MS detection of TDP-43 was conducted by comparison of the LC-MS/MS analysis of endogenous TDP-43 in HeLa cell with and without the use of the developed aptamer enrichment protocol (note the latter workflow is referred to herein as direct detection). LC-MS/MS analysis identified five and six monitored peptides by direct detection and aptamer enrichment, respectively (Figure 15). Compared to direct detection, aptamer enrichment yielded higher S/N with all six monitored peptides passing the detection criteria, including $TDP_{252-263}$, which was used for quantification of total TDP-43. LC-MS/MS analysis of aptamer-enriched TDP-43 from HeLa cell lysate resulted in a reported concentration of 0.60 ± 0.02 ng/mL.

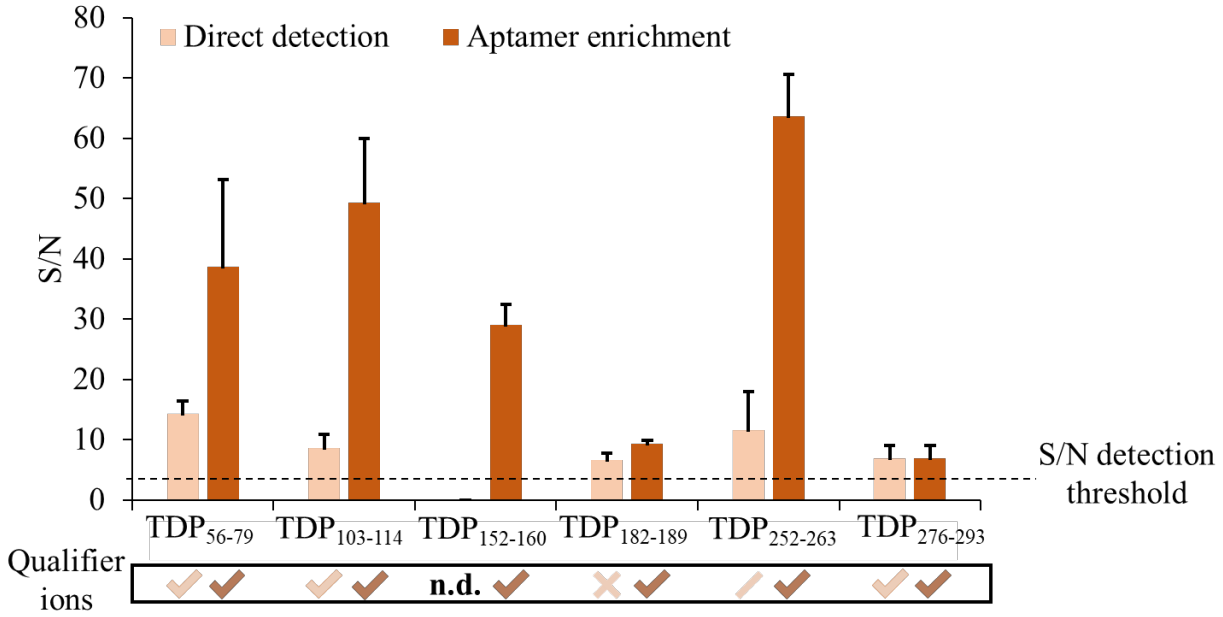

Figure 15: LC-MS/MS sequence coverage from neat HeLa cell lysate and post-aptamer enrichment (qualifier ion ratios: check = pass; single bar = one failed; "X" = both failed; and n.d. = not detected).

3.3.5 Aptamer Enrichment of Endogenous TDP-43 from Human Brain Tissue

Previously prepared homogenate supernatants from an unaffected individual and an individual with FTLD-TDP type A were analyzed by western blot and LC-MS/MS after in-gel digestion [50]. The soluble fractions of the same specimens were subjected to aptamer enrichment, instead of in-gel digestion, before being analyzed by LC-MS/MS. Upon in-gel digestion, five peptides were identified in both specimens, where only $TDP_{103\text{-}114}$ met the detection criteria (Figure 16). In contrast, all six monitored peptides were identified post-aptamer enrichment, with only $TDP_{103\text{-}114}$ of the unaffected specimen failing detection due to a qualifier ion ratio falling outside the expected peak area ratio. Aptamer enrichment led to improved S/N and increased TDP-43 sequence coverage, compared to in-gel digestion, upstream of LC-MS/MS analysis.

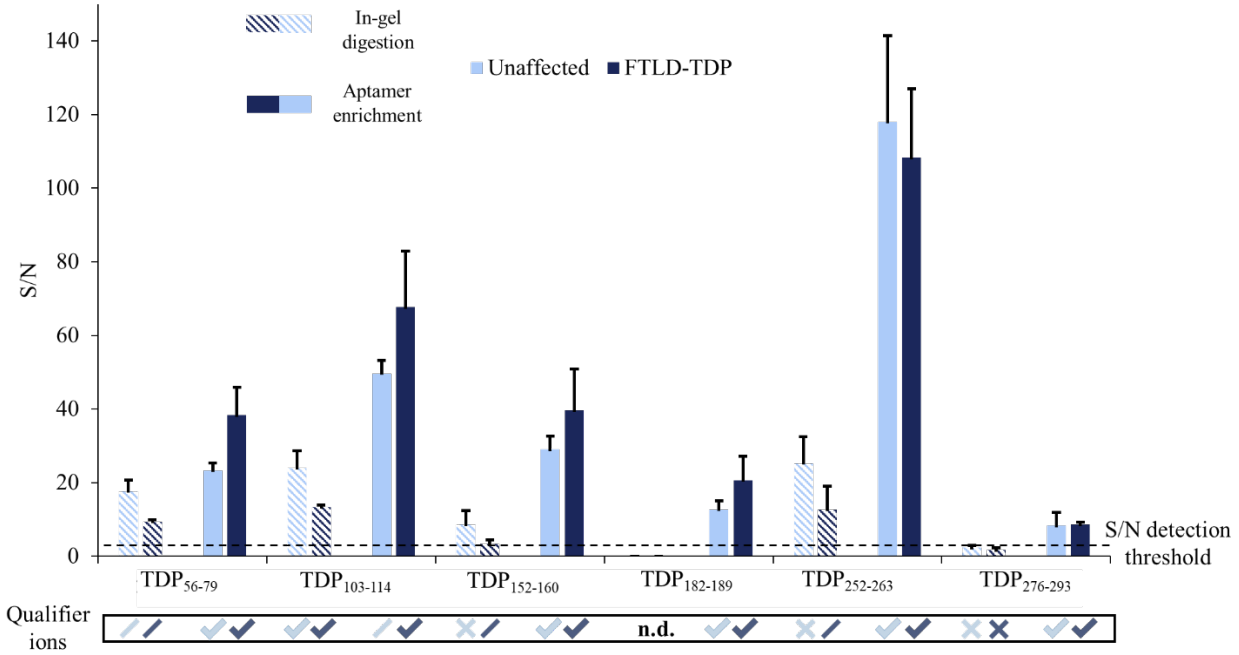

Figure 16: LC-MS/MS sequence coverage from human brain tissue specimens by in-gel digestion and post-aptamer enrichment (qualifier ion ratios: check = pass; single bar = one failed; "X" = both failed; and n.d. = not detected).

3.4 Discussion

The discovery of TDP-43 as the major pathological protein in the majority of FTD and ALS cases has led to continued focus on this protein toward a better understanding of TDP-43-related pathogenesis. With interest in detecting, characterizing and quantifying TDP-43, techniques of enrichment have been applied to remove background and increase protein concentration; most notably, immunoprecipitation. With multiple reports in literature noting cross-reactivity between anti-TDP antibodies with albumin and IgG [24-26], there is cause for concern when relying on immunometric methods. Furthermore, we have also observed cross-reactivity with IgG heavy chain from pooled human IVIg, and similar faint molecular weight banding when probing human

biofluids. This cross-reactivity with human IgG makes interpretation of the faint banding in the CSF and plasma difficult, where the presence of endogenous IgG could easily be mistaken for TDP-43. Towards a goal of seeking alternate forms of enrichment, we have developed an aptamer-based enrichment technique to improve the detection of TDP-43 in lower concentration solutions, prior to analysis. Through aptamer enrichment, the observed cross-reactivity with immunoprecipitation substrate during methods of immunoenrichment was removed, reducing the possibility for misinterpretation of results.

Calibration of the mass spectrometry quantification of TDP-43 was done by use of an internal heavy-labeled peptide calibrator. Using aptamer enrichment, measured TDP-43 concentrations of 1.10 ± 0.07 ng/mL and 0.62 ± 0.02 ng/mL were determined for HEK and HeLa cell lysates, respectively. These concentrations were supported by western blot findings, where banding of TDP-43 was roughly twice as dense in HEK cells compared to HeLa cells. While multi-point external calibration has long been the gold-standard for building quantitative bioanalytical assays, single-point calibration is gaining traction due to factors such as cost, time, and performance. In short, direct quantification during LC-MS/MS analysis with an internal calibrator can be done by using the analyte to stable isotope ratio [52]. In addition, the stable isotope labeled calibrator can serve as an IS to compensate for matrix effects during analysis such as chromatographic separation and ion suppression or enhancement. A systematic comparison of the bias and precision obtained between multi- and single-point calibration has been conducted in order to evaluate the two methods. For quantification of drugs in human plasma, the authors concluded that for the majority of analytes tested, an single-point internal calibrator was a feasible alternative to an external calibration curve [53]. In quantitative methods

involving upstream enrichment, internal single point calibrators have also been used. In one study, authors conducted an affinity enrichment of lipoproteins, where upon digestion, heavy-labeled IS peptides were added immediately prior to LC-MRM analysis and served as a single-point calibrator [54]. Here, we found that use of a single-point internal calibrator achieved a total CV of 15.6%. Analysis of the precision study data showed notable variation in the IS signal intensity. This variation could be due to the pre-analytical step whereby only a small volume (1.7 µl) of IS is spiked into the peptide digest immediately prior to analysis. Spiking in a greater volume of IS could reduce the variation in actual solution that is aspirated by the pipette and presents an opportunity to improve the CV.

We found that when using TDP-43 aptamer enrichment from human cells, it resulted in a lower complexity eluate as compared to immunoenrichment. This is beneficial as enrichment of TDP-43 can be applied upstream of many analytical approaches where reduced background interference is desired. Aptamer enrichment of TDP-43 coupled to detection by LC-MS/MS also showed a decrease in background signal compared to no enrichment, supporting western blot data. As a proof of concept, we applied the enrichment method to a previously homogenized soluble fraction of human brain tissue with western blot confirmed presence of TDP-43. The goal of improving sequence coverage was achieved with the use of aptamer enrichment prior to LC-MS/MS analysis.

We exploited the RNA-binding function of TDP-43 to develop an RNA aptamer-based enrichment strategy using an oligonucleotide sequence with a reported binding affinity in the low nanomolar range [49], consistent with that of high affinity antibodies used in techniques such as

immunoprecipitation and immunohistochemistry [55]. In addition to their stability, the low production cost to generate and synthesize aptamers is a major advantage compared to the development of antibodies, as no animals are needed [56]. Other benefits of aptamers over antibodies include the easiness of chemical modification as well as non-immunogenic properties. However, aptamers are not without their challenges (e.g., nuclease degradation), which must be accounted for during experimental design [48].

3.5 Conclusion

In general, the low abundance of TDP-43 in human biological matrices poses a challenge for detection. In addition, the cross-reactivity observed when using anti-TDP antibodies for both detection and quantification purposes can lead to misinterpretation of TDP-43 banding during western blot analyses, and falsely calculated analyte concentrations from immunometric methods, respectively. By developing an aptamer enrichment method for TDP-43, and the coupling to MRM LC-MS/MS detection, improved routine characterization of TDP-43 in human cell lines and tissues, was achieved. Exploiting the RNA-binding function of TDP-43 lead to an improved enrichment protocol relative to immunoenrichment. The method demonstrated selectivity for TDP-43 in human cell lines and tissues, and high sequence resolution.

Summary

To date, the detection of TDP-43 has relied primarily on immunometric approaches. Limitations of this approach include lack of specificity of commercially available anti-TDP antibodies, and that the recognition of a one or two epitopes on TDP-43 confers little information on the structure of the isoform of TDP-43 being detected. The developed LC-MS/MS method was able to structurally characterize TDP-43 by detection and/or absence of proteotypic peptides spanning different domains along the protein sequence. LC-MS/MS analysis of a human cell line identified five peptides spanning the TDP-43 sequence, where four peptides satisfied the detection criteria. LC-MS/MS analysis of unaffected and pathological brain tissue also identified five peptides, where two peptides for each tissue type satisfied the detection criteria. While we were able to identify 5 of our 6 monitored peptides in both cells and brain tissue, a number of peptides failed to meet the detection criteria. To improve detection and sequence coverage using the LC-MS/MS method, the sensitivity needed to be increased, which lead to our second aim of TDP-43 enrichment.

To increase the sensitivity of the newly developed LC-MS/MS detection method, we developed an RNA-based aptamer method of enrichment. The aptamer workflow showed successful enrichment of TDP-43 from human cell lines upon western blot analysis. Aptamer enrichment of TDP-43 from human cell lines coupled to LC-MS/MS analysis successfully detected all six monitored peptides, demonstrating increased sensitivity compared to direct detection of TDP-43. A similar increase in detection sensitivity was noted for analyses of human brain tissues. For quantification, a single point internal calibrator was used. With successful enrichment from human cells and tissues, this method demonstrated improved sensitivity compared to direct

detection of TDP-43 in biological matrices, as well as increased specificity of the enrichment process compared to immunoenrichment, when applied upstream of LC-MS/MS.

References

[1] Ou SH, Wu F, Harrich D, Garcia-Martinez LF, Gaynor RB (1995). Cloning and characterization of a novel cellular protein, TDP-43, that binds to human immunodeficiency virus type 1 TAR DNA sequence motifs. J Virol 69: 3584-3596

[2] Wang HY, Wang IF, Bose J, Shen CK (2004). Structural diversity and functional implications of the eukaryotic TDP gene family. Genomics 83: 130-139

[3] Buratti E, Dork T, Zuccato E, Pagani F, Romano M, Baralle FE (2001). Nuclear factor TDP-43 and SR proteins promote in vitro and in vivo CFTR exon 9 skipping. The EMBO journal 20: 1774-1784

[4] Ayala YM, Zago P, D'Ambrogio A, Xu YF, Petrucelli L, Buratti E, Baralle FE (2008). Structural determinants of the cellular localization and shuttling of TDP-43. J. Cell. Sci. 121: 3778-3785

[5] Buratti E, Baralle FE (2001). Characterization and functional implications of the RNA binding properties of nuclear factor TDP-43, a novel splicing regulator of CFTR exon 9. J. Biol. Chem 276: 36337-36343

[6] Rogelj B, Godin KS, Shaw CE, A Ule J (2011) The functions of the glycine-rich regions in TDP-43, FUS and related RNA-binding proteins. RNA Binding Proteins. 9781587066566

[7] Budini M, Buratti E, Stuani C, Guarnaccia C, Romano V, De Conti L, Baralle FE (2012). Cellular model of TAR DNA-binding protein 43 (TDP-43) aggregation based on its C-terminal Gln/Asn-rich region. J. Biol. Chem 287: 7512-7525

[8] Strong MJ, Volkening K, Hammond R, Yang W, Strong W, Leystra-Lantz C, Shoesmith C (2007). TDP43 is a human low molecular weight neurofilament (hNFL) mRNA-binding protein. Mol. Cell. Neurosci. 35: 320-327

[9] Kawahara Y, Mieda-Sato A (2012). TDP-43 promotes microRNA biogenesis as a component of the Drosha and Dicer complexes. Proc Natl Acad Sci U S A 109: 3347-3352

[10] Mackenzie IR, Rademakers R, Neumann M (2010). TDP-43 and FUS in amyotrophic lateral sclerosis and frontotemporal dementia. Lancet. Neurol. 9: 995-1007

[11] Onyike CU, Diehl-Schmid J (2013). The epidemiology of frontotemporal dementia. Int Rev Psychiatry 25: 130-137

[12] Rabinovici GD, Miller BL (2010). Frontotemporal lobar degeneration: epidemiology, pathophysiology, diagnosis and management. CNS drugs 24: 375-398

[13] Brown RH, Al-Chalabi A (2017). Amyotrophic lateral sclerosis. The New England journal of medicine 377: 162-172

[14] Chio A, Logroscino G, Traynor BJ, Collins J, Simeone JC, Goldstein LA, White LA (2013). Global epidemiology of amyotrophic lateral sclerosis: a systematic review of the published literature. Neuroepidemiology 41: 118-130

[15] Mackenzie IR, Baborie A, Pickering-Brown S, Du Plessis D, Jaros E, Perry RH, Neary D, Snowden JS, Mann DM (2006). Heterogeneity of ubiquitin pathology in frontotemporal lobar degeneration: classification and relation to clinical phenotype. Acta Neuropathol 112: 539-549

[16] Sampathu DM, Neumann M, Kwong LK, Chou TT, Micsenyi M, Truax A, Bruce J, Grossman M, Trojanowski JQ, Lee VM (2006). Pathological heterogeneity of frontotemporal lobar degeneration with ubiquitin-positive inclusions delineated by ubiquitin immunohistochemistry and novel monoclonal antibodies. Am J Pathol 169: 1343-1352

[17] Strong MJ, Kesavapany S, Pant HC (2005). The pathobiology of amyotrophic lateral sclerosis: a proteinopathy? Journal of neuropathology and experimental neurology 64: 649-664

[18] Neumann M, Sampathu DM, Kwong LK, Truax AC, Micsenyi MC, Chou TT, Bruce J, Schuck T, Grossman M, Clark CM, McCluskey LF, Miller BL, Masliah E, Mackenzie IR, Feldman H, Feiden W, Kretzschmar HA, Trojanowski JQ, Lee VMY (2006). Ubiquitinated TDP-43 in frontotemporal lobar degeneration and amyotrophic lateral sclerosis. Science 314: 130

[19] Arai T, Hasegawa M, Akiyama H, Ikeda K, Nonaka T, Mori H, Mann D, Tsuchiya K, Yoshida M, Hashizume Y, Oda T (2006). TDP-43 is a component of ubiquitin-positive tau-negative inclusions in frontotemporal lobar degeneration and amyotrophic lateral sclerosis. Biochem. Biophys. Res. Commun. 351: 602-611

[20] Mackenzie IR, Neumann M, Bigio EH, Cairns NJ, Alafuzoff I, Kril J, Kovacs GG, Ghetti B, Halliday G, Holm IE, Ince PG, Kamphorst W, Revesz T, Rozemuller AJ, Kumar-Singh S, Akiyama H, Baborie A, Spina S, Dickson DW, Trojanowski JQ, Mann DM (2009). Nomenclature for neuropathologic subtypes of frontotemporal lobar degeneration: consensus recommendations. Acta Neuropathol 117: 15-18

[21] Hasegawa M, Arai T, Nonaka T, Kametani F, Yoshida M, Hashizume Y, Beach TG, Buratti E, Baralle F, Morita M, Nakano I, Oda T, Tsuchiya K, Akiyama H (2008). Phosphorylated TDP-43 in frontotemporal lobar degeneration and amyotrophic lateral sclerosis. Ann. Neurol. 64: 60-70

[22] Neumann M (2009). Molecular neuropathology of TDP-43 proteinopathies. Int. J. Mol. Sci. 10: 232-246

[23] Neumann M, Tolnay M, Mackenzie IR (2009). The molecular basis of frontotemporal dementia. Expert. Rev. Mol. Med. 11: e23

[24] Feneberg E, Steinacker P, Lehnert S, Schneider A, Walther P, Thal DR, Linsenmeier M, Ludolph AC, Otto M (2014). Limited role of free TDP-43 as a diagnostic tool in neurodegenerative diseases. Amyotroph. Lateral. Scler. Frontotemporal. Degener. 15: 351-356

[25] Kasai T, Tokuda T, Ishigami N, Sasayama H, Foulds P, Mitchell DJ, Mann DM, Allsop D, Nakagawa M (2009). Increased TDP-43 protein in cerebrospinal fluid of patients with amyotrophic lateral sclerosis. Acta. Neuropathol. 117: 55-62

[26] Steinacker P, Hendrich C, Sperfeld AD, Jesse S, von Arnim CA, Lehnert S, Pabst A, Uttner I, Tumani H, Lee VM, Trojanowski JQ, Kretzschmar HA, Ludolph A, Neumann M, Otto M (2008). TDP-43 in cerebrospinal fluid of patients with frontotemporal lobar degeneration and amyotrophic lateral sclerosis. Arch. Neurol. 65: 1481-1487

[27] Zheng YZ, DeMarco ML (2017). Manipulating trypsin digestion conditions to accelerate proteolysis and simplify digestion workflows in development of protein mass spectrometric assays for the clinical laboratory. Clinical Mass Spectrometry. 6: 1-12

[28] MacLean B, Tomazela DM, Shulman N, Chambers M, Finney GL, Frewen B, Kern R, Tabb DL, Liebler DC, MacCoss MJ (2010). Skyline: an open source document editor for creating and analyzing targeted proteomics experiments. Bioinformatics (Oxford, England) 26: 966-968

[29] Holmes DT (2015). cp-R, an interface the R programming language for clinical laboratory method comparisons. Clin. Biochem. 48: 192-195

[30] Hendriks IA, Lyon D, Young C, Jensen LJ, Vertegaal AC, Nielsen ML (2017). Site-specific mapping of the human SUMO proteome reveals co-modification with phosphorylation. Nat. Struct. Mol. Biol. 24: 325-336

[31] Zhou H, Di Palma S, Preisinger C, Peng M, Polat AN, Heck AJ, Mohammed S (2013). Toward a comprehensive characterization of a human cancer cell phosphoproteome. J. Proteome. Res. 12: 260-271

[32] Guo A, Gu H, Zhou J, Mulhern D, Wang Y, Lee KA, Yang V, Aguiar M, Kornhauser J, Jia X, Ren J, Beausoleil SA, Silva JC, Vemulapalli V, Bedford MT, Comb MJ (2014). Immunoaffinity enrichment and mass spectrometry analysis of protein methylation. Mol. Cell. Proteomics. 13: 372-387

[33] Moreno F, Rabinovici GD, Karydas A, Miller Z, Hsu SC, Legati A, Fong J, Schonhaut D, Esselmann H, Watson C, Stephens ML, Kramer J, Wiltfang J, Seeley WW, Miller BL, Coppola G, Grinberg LT (2015). A novel mutation P112H in the TARDBP gene associated with frontotemporal lobar degeneration without motor neuron disease and abundant neuritic amyloid plaques. Acta Neuropathol Commun 3: 19

[34] Fang YS, Tsai KJ, Chang YJ, Kao P, Woods R, Kuo PH, Wu CC, Liao JY, Chou SC, Lin V, Jin LW, Yuan HS, Cheng IH, Tu PH, Chen YR (2014). Full-length TDP-43 forms toxic amyloid oligomers that are present in frontotemporal lobar dementia-TDP patients. Nat. Commun. 5: 4824

[35] Dawson TM, Golde TE, Lagier-Tourenne C (2018). Animal models of neurodegenerative diseases. Nature Neurosci. 21: 1370-1379

[36] Igaz LM, Kwong LK, Chen-Plotkin A, Winton MJ, Unger TL, Xu Y, Neumann M, Trojanowski JQ, Lee VM (2009). Expression of TDP-43 C-terminal fragments in vitro recapitulates pathological features of TDP-43 proteinopathies. J. Biol. Chem 284: 8516-8524

[37] Ling SC, Albuquerque CP, Han JS, Lagier-Tourenne C, Tokunaga S, Zhou H, Cleveland DW (2010). ALS-associated mutations in TDP-43 increase its stability and promote TDP-43 complexes with FUS/TLS. Proc Natl Acad Sci U S A 107: 13318-13323

[38] Newell K, Paron F, Mompean M, Murrell J, Salis E, Stuani C, Pattee G, Romano M, Laurents D, Ghetti B, Buratti E (2018). Dysregulation of TDP-43 intracellular localization and early onset ALS are associated with a TARDBP S375G variant. Brain. Pathol. 29: 397-413

[39] Zhang YJ, Xu YF, Dickey CA, Buratti E, Baralle F, Bailey R, Pickering-Brown S, Dickson D, Petrucelli L (2007). Progranulin mediates caspase-dependent cleavage of TAR DNA binding protein-43. J. Neurosci. 27: 10530-10534

[40] Dormann D, Capell A, Carlson AM, Shankaran SS, Rodde R, Neumann M, Kremmer E, Matsuwaki T, Yamanouchi K, Nishihara M, Haass C (2009). Proteolytic processing of TAR DNA binding protein-43 by caspases produces C-terminal fragments with disease defining properties independent of progranulin. J. Neurochem. 110: 1082-1094

[41] Zhang YJ, Xu YF, Cook C, Gendron TF, Roettges P, Link CD, Lin WL, Tong J, Castanedes-Casey M, Ash P, Gass J, Rangachari V, Buratti E, Baralle F, Golde TE, Dickson DW, Petrucelli L (2009). Aberrant cleavage of TDP-43 enhances aggregation and cellular toxicity. Proc. Natl. Acad. Sci. U. S. A. 106: 7607-7612

[42] Ackermann BL (2012). Understanding the role of immunoaffinity-based mass spectrometry methods for clinical applications. Clinical chemistry 58: 1620-1622

[43] Hoofnagle AN, Wener MH (2009). The fundamental flaws of immunoassays and potential solutions using tandem mass spectrometry. J Immunol Methods 347: 3-11

[44] Keefe AD, Pai S, Ellington A (2010). Aptamers as therapeutics. Nat Rev Drug Discov 9: 537-550

[45] Parashar A (2016). Aptamers in therapeutics. Journal of Clinical and Diagnostic Research : JCDR 10: BE01-BE06

[46] Kaur H, Bruno JG, Kumar A, Sharma TK (2018). Aptamers in the therapeutics and diagnostics pipelines. Theranostics 8: 4016-4032

[47] Ptitsyn KG, Novikova SE, Kiseleva YY, Moysa AA, Kurbatov LK, Farafonova TE, Radko SP, Zgoda VG, Archakov AI (2018). Use of DNA-aptamers for enrichment of low abundant proteins in cellular extracts for quantitative detection by selected reaction monitoring. Biochemistry (Moscow), Supplement Series B: Biomedical Chemistry 12: 176-180

[48] Lakhin AV, Tarantul VZ, Gening LV (2013). Aptamers: problems, solutions and prospects. Acta Naturae 5: 34-43

[49] Bhardwaj A, Myers MP, Buratti E, Baralle FE (2013). Characterizing TDP-43 interaction with its RNA targets. Nucleic Acids Res 41: 5062-5074

[50] Pobran TD, Forgrave LM, Zheng YZ, Lim JGK, Mackenzie IRA, DeMarco ML (2019). Detection and characterization of TDP-43 in human cells and tissues by multiple reaction monitoring mass spectrometry. Clinical Mass Spectrometry 14: 66-73

[51] CLSI (2014). C62-A Liquid Chromatography-Mass Spectrometry Methods; Approved Guideline.

[52] Nilsson LB, Eklund G (2007). Direct quantification in bioanalytical LC-MS/MS using internal calibration via analyte/stable isotope ratio. Journal of pharmaceutical and biomedical analysis 43: 1094-1099

[53] Peters FT, Maurer HH (2007). Systematic comparison of bias and precision data obtained with multiple-point and one-point calibration in six validated multianalyte assays for quantification of drugs in human plasma. Analytical chemistry 79: 4967-4976

[54] Jin Z, Collier TS, Dai DLY, Chen V, Hollander Z, Ng RT, McManus BM, Balshaw R, Apostolidou S, Penn MS, Bystrom C (2019). Development and validation of apolipoprotein AI-associated lipoprotein proteome panel for the prediction of cholesterol efflux capacity and coronary artery disease. Clinical chemistry 65: 282-290

[55] Liu S, Zhang H, Dai J, Hu S, Pino I, Eichinger DJ, Lyu H, Zhu H (2015). Characterization of monoclonal antibody's binding kinetics using oblique-incidence reflectivity difference approach. MAbs 7: 110-119

[56] Song K-M, Lee S, Ban C (2012). Aptamers and their biological applications. Sensors (Basel) 12: 612-631